Theor Chem Acc (2001) 105:328–337
DOI 10.1007/s002140000231

Theoretical
Chemistry Accounts

Regular article

The three-center-four-electron (3c-4e) bond nature revisited. An atoms-in-molecules theory (AIM) and ELF study

José Molina Molina, José A. Dobado

Grupo de Modelización y Diseño Molecular, Instituto de Biotecnología, Campus Fuentenueva s/n, Universidad de Granada, 18071-Granada, Spain, e-mail: dobado@ugr.es; Tel.: +34-958-243186; Fax: +34-958-243186

Received: 1 June 2000 / Accepted: 4 October 2000 / Published online: 19 January 2001

Abstract. Theoretical calculations (B3LYP/6–311++G**) were performed on a series of formally hypervalent compounds showing linear three-center geometries. The bonding nature was analyzed by the electron density, $\rho(r)$, and electron-localization function (ELF) topologies, including calculations of the AIM charges and NMR chemical shifts (GIAO method). In addition, a quantitative analysis was also performed of the localization and delocalization indexes, obtained from the electron-pair density in conjunction with the definition of an atom in a molecule. Furthermore, the populations and fluctuations in the ELF basins were also evaluated. The compounds studied presented linear (**1–5**), T-shaped (**6–9**), and bipyramidal structures (**10–15**). Our results support the 3c-4e model for the linear (**1–5**) structures, but reveal for the T-shaped (**6–9**) structures only a small contribution from this model. In addition, there is no evidence to support the 3c-4e bond scheme for the bipyramidal compounds (**10–15**).

Key words: *Ab initio* calculations – Atoms-in-molecules – Bond theory – Three-center-four-electron bond – Electron localization function

1 Introduction

The bond nature in hypervalent compounds has long been controversial, and has been the object of several recent reviews [1, 2]. Special attention has been focused on chalcogen oxides [3] and ylides [4]. Historically, the bonding nature for these compounds has been based on an sp^xd^y hybridization scheme. However, it is now clear from accurate *ab initio* calculations that *d* orbitals do not participate in bonding, but act solely as polarization functions [1, 5]. The bonding schemes presented in the literature for hypervalent compounds arise from different analyses of the electronic wave function, indicating the importance of a rigorous and observation-based interpretation of the theoretical results [6]. The bonding properties of different linear, three-center hypervalent compounds have been characterized by the Rundle [7] and Pimentel [8] three-center-four-electron model (3c-4e). The application of this model to the $[F_3]^-$ molecule is depicted in Fig. 1.

A valence bond description of the 3c-4e scheme was performed by Linnett [9]. The 3c-4e model postulates three MOs, Ψ_1 with bonding nature, Ψ_3 with antibonding, and Ψ_2 with no bonding character. These three MOs yield an overall bond order of 0.5 with two electrons almost localized on the external fluorines with atomic charges of -0.5 e$^-$. This scheme has also been extended to other hypervalent molecules such as F_3Cl, $[F_3S]^-$, F_4S, F_5P, $[F_5Si]^-$ or F_6S, with different trigonal-bipyramid or octahedral geometries. Furthermore, an explanation of the dissimilar ligand equatorial and axial bond lengths to the central atom is rationalized by these geometrical arrangements. Another point of view in the description of these hypervalent structures is the Generalized Valence Bond approach summarized by the *democracy principle* proposed by Cooper et al. [10], in which a particular atom uses any of its valence electrons in the chemical bonding, based on the principle of minimizing the total energy.

In recent years, an observation-based interpretative tool has been extensively used, the atoms-in-molecules (AIM) theory [11]. In this context, AIM has been used in the bonding description of different hypervalent compounds [3,4a,6,12]. A complementary method to study the chemical bonding is the electron-localization function (ELF) [13] analysis of Becke and Edgecombe [14]. Moreover, the ELF topological analysis has been also used to define chemical bonding including that in hypervalent molecules [12].

An appropriate definition of bonding indexes is of great importance for the bonding characterization of

This work is dedicated to Professor Serafín Fraga
Professor José Molina Molina passed away on the 13th June 2000
Contribution to the Proceedings of the 2000 Symposium on Chemical Bonding: State of the Art in Conceptual Quantum Chemistry.

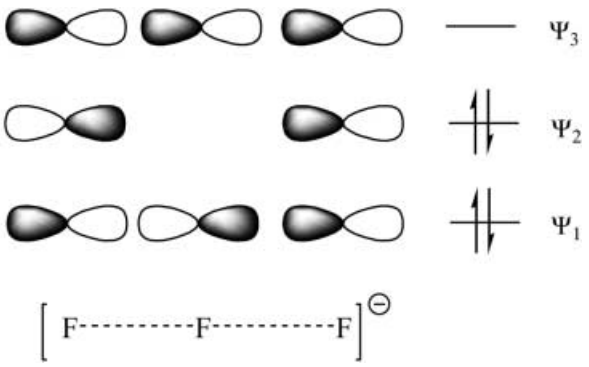

Fig. 1. Schematic molecular orbitals for the 3c-4e bond model of $[F_3]^-$ molecule

hypervalent compounds [15]. Therefore, much effort has been made in the past to define such a non-observable concept of chemical bonding [15, 16]. The corresponding covalent bond orders were defined both in the HF context or at the correlated level, while addressing the necessity of using the AIM atomic basins in the population analysis [16]. Moreover, other multi-center bond indexes have been proposed to study the 3c-4e model in the context of hypervalent molecules [17]. Considering that the bond is a non-observable concept in the Quantum Chemistry definition, electron-delocalization indexes have also been defined based on the pair density to link Quantum Mechanical and Classical approaches to chemical structures. This definition was made [18] using the Mulliken approximation to define charge density, bond order, etc., yielding indexes equivalent to those of Wiberg [19].

Another alternative is the delocalization indexes formulated by integration of the pair density between the atomic basins defined by the AIM theory [20, 21]. In this work, the 3c-4e bond model is revisited based on an adequate topological analysis of ρ(r) and ELF, together with the electron delocalization indexes proposed by Bader, and the theoretical NMR chemical shifts. The study has been performed for the hypervalent compounds depicted in Figs. 2 and 3. Geometrical and electronic calculations for **1**–**15** have already been extensively reported in the literature [22], including their ρ(r) and ELF analyses [12], and the results are compatible with the VSEPR model [23].

2 Computational details

General methods

Density functional theory (B3LYP) calculations were performed with the Gaussian 98 package of programs [24]. All the minimum structures were fully optimized and tested by frequency analysis at the B3LYP/6-311++G** level, yielding the minima with constrained symmetries (see Figs. 2 and 3) and non-imaginary frequencies. The AIM analysis [11] has been performed with the AIMPAC series of programs [25], using the DFT densities as the input.

The NMR chemical shifts were calculated by the GIAO method [26] using the tetramethylsilane (TMS) shielding as references for the ^{1}H ($\delta_{\mathbf{H}}$) chemical shift (31.98 ppm).

The $\nabla^2\rho$(r) contour-map representations have been produced using the MORPHY98 program [27]. The ELF analyses have been made with the ToPMoD package of programs [28].

Overview of the $\rho(r)$ and ELF topologies

The topology of the electronic charge density, ρ(r), as pointed out by Bader [11], is an accurate mapping of the chemical concepts of atoms, bonds, and structures. The principal topological properties are summarized in terms of their critical points (CP) [11], and the nuclear positions behave topologically as local maxima in ρ(r). A bond critical point (BCP) is found between each pair of nuclei, which are considered to be linked by a chemical bond, with two negative curvatures, (λ_1 and λ_2) and one positive (λ_3) [denoted as (3, −1) CP]. The ellipticity, ε, of a bond is defined by means of the two negative curvatures in a BCP as:

$$\varepsilon = \lambda_1/\lambda_2 - 1, \qquad \text{where } |\lambda_2| < |\lambda_1| \tag{1}$$

The ring CPs are characterized by a single negative curvature. Each (3, −1) CP generates a pair of gradient paths [11] which originate at a CP and terminate at neighboring attractors. This gradient path defines a line through the charge distribution linking the neighboring nuclei. Along this line, ρ(r) is a maximum with respect to any neighboring line. Such a line is referred to as an atomic interaction line [11]. The presence of an atomic-interaction line in such equilibrium geometry satisfies both the necessary and sufficient conditions that the atoms be bonded together.

The Laplacian of the electronic charge density, $\nabla^2\rho$(r), describes two extreme situations. In the first, ρ(r) is locally concentrated [$\nabla^2\rho(r) < 0$] and in the second it is locally depleted [$\nabla^2\rho(r) > 0$]. Thus, a value of $\nabla^2\rho(r) < 0$ at a BCP is unambiguously related to a covalent bond, showing that a sharing of charge has taken place. In a closed-shell interaction, a value of $\nabla^2\rho(r) > 0$ is expected, as found in noble gas repulsive states, ionic bonds, hydrogen bonds, and van der Waals molecules. Bader has also defined a local electronic energy density, E_d(r), as a function of the first-order density matrix:

$$E_d(r) = G(r) + V(r) \tag{2}$$

where the G(r) and V(r) correspond to a local kinetic and potential energy density, respectively [11]. The sign of the E_d(r) determines whether a charge accumulation at a given point r is stabilizing [$E_d(r) < 0$] or destabilizing [$E_d(r) > 0$]. Thus, a value of $E_d(r) < 0$ at a BCP presents a significant covalent contribution and, therefore, a lowering of the potential energy associated with the concentration of charge between the nuclei.

The quantum-mechanical pair density in conjunction with the quantum definition of an atom in a molecule provides a precise determination of the extent to which electrons are localized in a given atom and delocalized over any pair of atoms [21]. The electron pairing is a consequence of the Pauli exclusion principle, and the extent of spatial localization of the pairing is determined by the corresponding property of the Fermi hole density. These ideas are made quantitative through the appropriate integration of the pair density to determine the total Fermi correlation contained within a single atomic basin, the quantity $F(A,A)$, or $F(A,B)$, the correlation shared between two basins. The quantity $F(A,B)$ is thus a measure of the extent to which electrons of either spin referenced to atom A are delocalized into atom B with a corresponding definition of $F(B,A)$. Thus, $F(B,A) = F(A,B)$ and their sum, $F(A,B) + F(B,A) = \delta(A,B)$, termed the *delocalization index*, is a measure of the total Fermi correlation shared between the atoms. This delocalization index is calculated taking into account that

$$F(A,B) = F(B,A) = -\sum_i \sum_j - S_{ij}(A) \cdot S_{ij}(B) \tag{3}$$

where S_{ij}(A) is the corresponding atomic overlap matrix given by the PROAIM program at the Hartree-Fock level [20].

The ELF function [13, 14], which was first introduced by Becke and Edgecombe [14], can be viewed as a local measure of the Pauli repulsion between electrons due to the exclusion principle, enabling us to define regions of space that are associated with different electron pairs. The ELF function is expressed by

$$ELF = \frac{1}{1 + \left(\frac{D}{D_h}\right)^2} \tag{4}$$

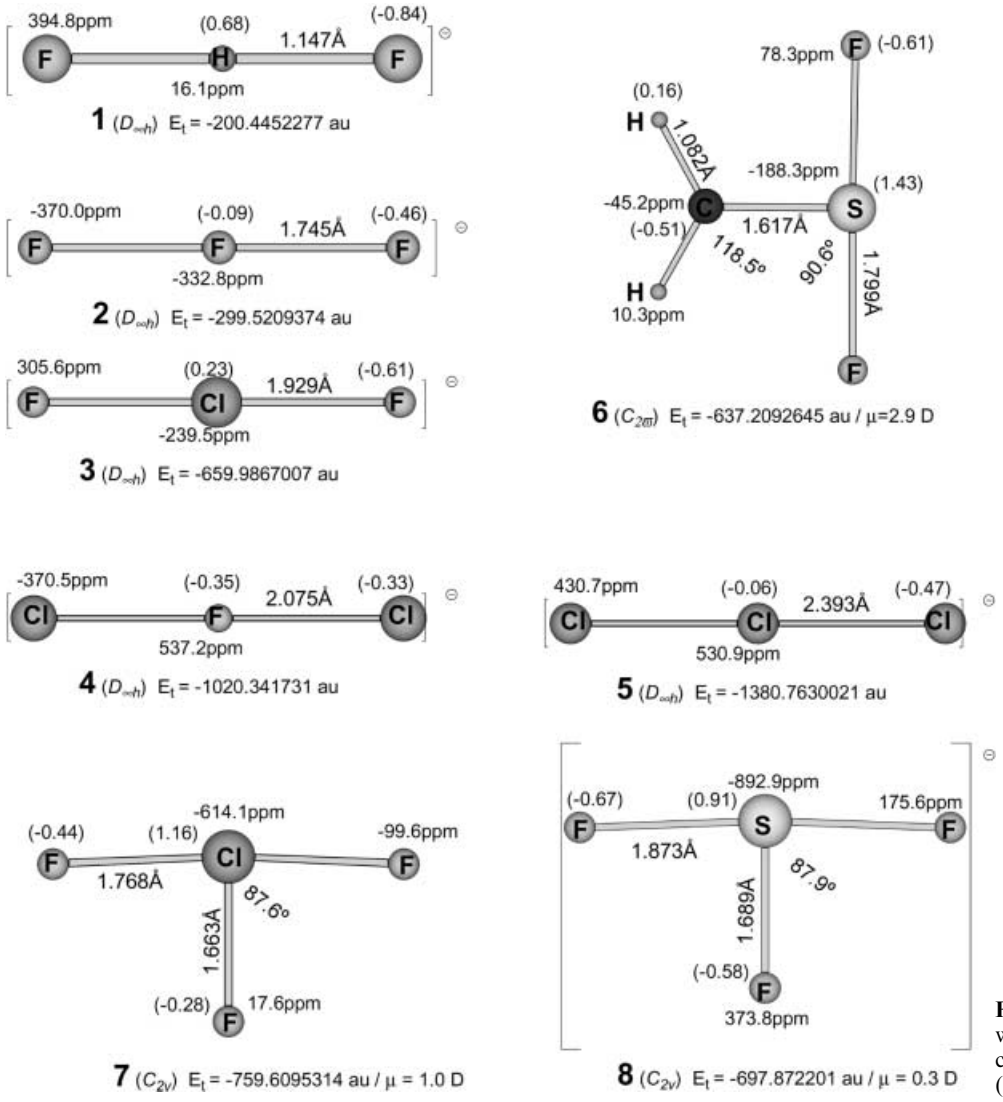

Fig. 2. Hypervalent structures (**1**–**8**) with the geometrical parameters, charges and NMR chemical shifts, (in parentheses symmetry)

where

$$D = \frac{1}{2}\sum_{j=1}^{N}\left|\nabla\varphi_j\right|^2 - \frac{1}{8}\frac{|\nabla\rho|^2}{\rho};\quad D_h = \frac{3}{10}\left(3\pi^2\right)^{2/3}\rho^{5/3};\quad \rho = \sum_{j=1}^{N}\left|\varphi_j\right|^2 \tag{5}$$

This definition gives ELF values between 0 and 1, with large values where two anti-parallel spin electrons are paired in space and small ones in the regions between electron pairs. Considering the scalar character of the ELF function, the analysis of their gradient fields yields their attractors (local maxima) and their corresponding basins. There are two type of basins: the core basins labeled by C(atom symbol) and the valence basins V(list of atoms). The valence basins are characterized by their synaptic order (the number of core basins with which they share a common boundary). Accordingly, they can be classified as mono-, di- and polysynaptic, corresponding to the lone pair, bicentric and polycentric bonding region, respectively. The quantitative population on the different basins are calculated by integrating a given density of property over the volume of the basins. The following definitions are used through the text: basin population $\bar{N}(\Omega_i) = \int_{\Omega_i}\rho(r)dr$ and its variance $\sigma^2(\Omega_i) = \int_{\Omega_i}\int_{\Omega_i}\pi(r,r')drdr' + \bar{N}(\Omega_i) - \bar{N}^2(\Omega_i)$ % in which $\pi(r,r')$ is the two electron density, covariance $B_{ij} = \bar{N}(\Omega_i)\cdot\bar{N}(\Omega_j) - P(\Omega_i,\Omega_j)$ % in which $P(\Omega_i,\Omega_j)$ is the pair population, and the fluctuation contribution $\frac{B_{ij}}{\sum_{i\neq j}B_{ij}}$.

3 Results and discussion

Theoretical calculations have been performed on the structures depicted in Figs. 2 and 3 together with their corresponding reference non-hypervalent compounds (Fig. 4) at the B3LYP/6-311++G** theoretical level, which has proven its utility for describing accurate geometrical and electronic features in similar hypervalent derivatives [3, 4]. These figures illustrate the geometrical parameters, yielding geometries in agreement with the values reported in the literature. In general, the geometric and electronic behavior are compatible with the VSEPR molecular geometry model [23].

The topology of the electron density, ρ(r), has been analyzed following the AIM theory, yielding maxima of electron concentration also compatible with the VSEPR model. The numerical values at the different BCPs are

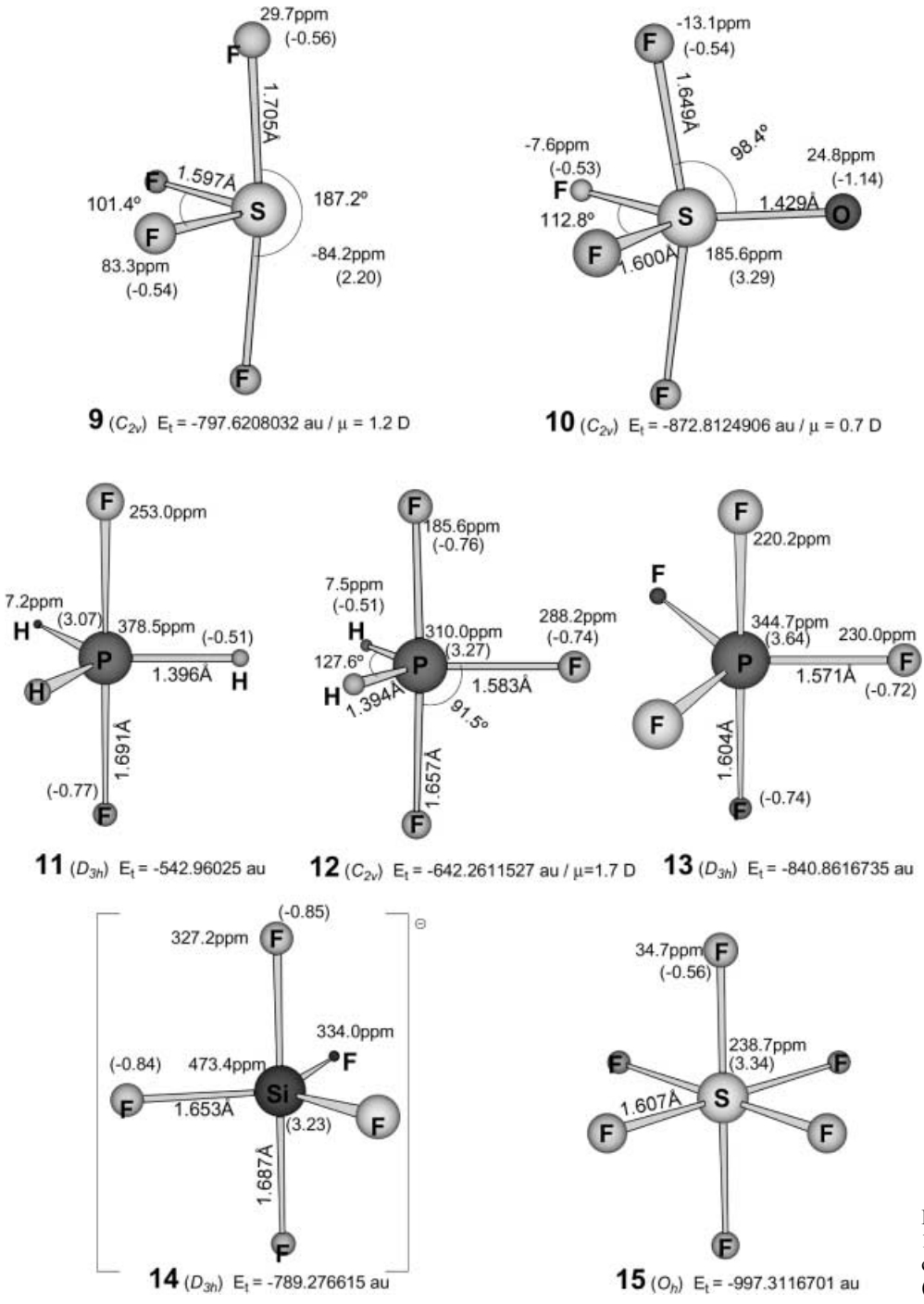

Fig. 3. Hypervalent structures (**9–15**) with the geometrical parameters, charges and NMR chemical shifts, (in parentheses symmetry)

depicted in Table 1. Integration of the density in the atomic basins gave the AIM atomic charges. Moreover, the GIAO method was used to generate the corresponding isotropic chemical shifts for the different atoms (see Figs. 2–4).

The following trends are extracted from the geometrical parameters and electronic properties.

1) The linear anionic structures (**1–5**) lengthened their bonds by more than 0.2 Å compared to the corresponding reference compounds (**16–19**). Furthermore, the main differences appeared in **4** with a F-Cl lengthening *ca.* 0.4 Å compared to **19**. The negative charge was located mainly on the two terminal atoms, giving a highly positive hydrogen atom in **1**, and an slightly positive chlorine atom in **3**. By contrast, the central atoms for **2** and **5** remained almost neutral. Moreover, for **4** the fluorine had a negative value and was similar to the terminal chlorines.
2) The T-shaped structures (**6–9**) (with lone pairs at the central atom) had larger fluorine axial bonds than the corresponding equatorial ones (>0.1 Å). However,

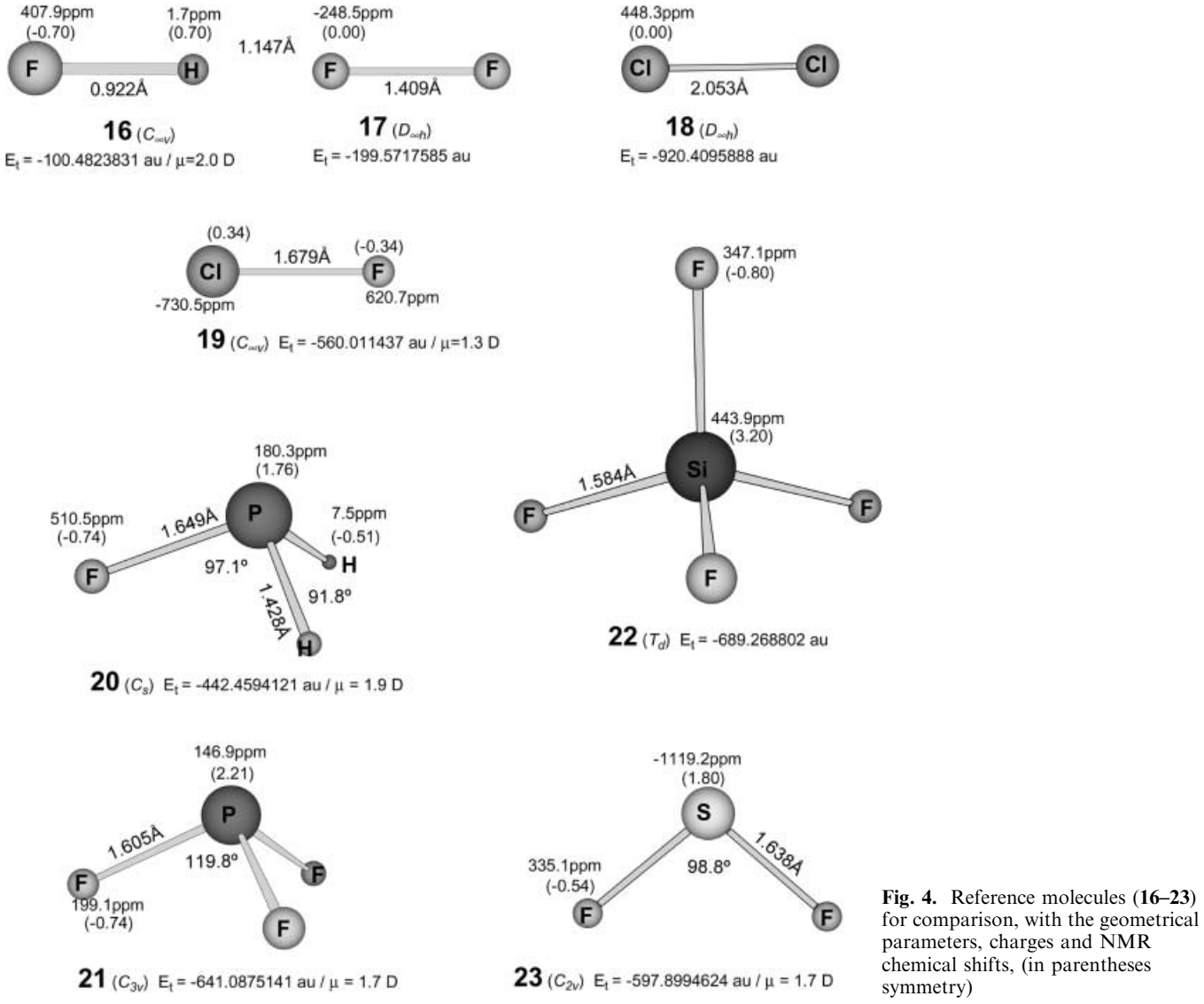

Fig. 4. Reference molecules (**16–23**) for comparison, with the geometrical parameters, charges and NMR chemical shifts, (in parentheses symmetry)

the differences with the reference compounds were shorter than in the linear structures.

3) The fluorine axial/equatorial bond length differences for **10**–**15** (without lone pairs at the central atom) were very small (< 0.08 Å).
4) The atomic charges on the F_a and F_e atoms were very similar for **7–15**; however, the largest difference was found for **7** (0.16 e^-).

The nature of the F-X bond has been analyzed, considering the $\rho(r)$ topology (see Table 1), yielding the linear structures (**1–5**) a very polar unstabilized behavior with small $\rho(r)$ values, positive $\nabla^2\rho(r)$, small λ_1/λ_3 and $E_d(r)$ values close to zero at the BCPs. However, structure **1** deviated from these trends due to the strong electrostatic interaction between the hydrogen and the two fluorines ($\rho(r) = 0.170$ e/a_o^3 and $\nabla^2\rho(r) = -0.29$ e/a_o^5). The sulfur derivatives enhanced the S-F covalent character, giving higher $\rho(r)$ and negative $\nabla^2\rho(r)$ values. In addition, the numerical values matched the geometrical results. The remaining structures with Cl (**7**), P (**11–13**) and Si (**14**) as the central atom displayed highly polar bonds, but with notable covalent character in accord with $\rho(r) > 0.1$ e/a_o^3 positive $\nabla^2\rho(r) > 0.35$ e/a_o^5 and negative $E_d(r)$ values. Furthermore, the differences in the numerical values for the axial/equatorial bonds were very small.

The ^{19}F-NMR chemical shifts were calculated to evaluate the differences in the chemical environment, giving the linear structures trends similar to the reference compounds. Moreover, the T-shaped structures (**6–9**) presented sharply different axial shifts (δ_{Fa}) compared to the equatorial values, the largest differences being found for structure **7** and **8** (> 100 ppm). The axial/equatorial differences were due mainly to the chemical environment of these compounds, with equatorial disposition for the central atom lone pairs. The largest differences in **7** and **8** are explained by the existence of two lone pairs, in contrast to the only one for **6** and **9**. The axial/equatorial shifts values were very similar for the structures without lone pairs on the central atom (**10–15**), excluding **12** which has another two equatorial hydrogens.

Table 1. Electronic charge density, $\rho(r)$, its Laplacian, $\nabla^2\rho(r)$, ellipticity, ε, curvatures, λ_1/λ_3, and electronic energy density, $E_d(r)$, at the B3LYP/6-311++G** theoretical level for the different BCPs

Structure	Bond	$\rho(r)$ (e/a_o^3)	$\nabla^2\rho(r)$ (e/a_o^5)	ε	$\lvert\lambda_1/\lambda_3\rvert$	$E_d(r)$ (Hartree/a_o^3)
1, FHF^-	F-H	0.174	−0.290	0.000	0.645	−0.186
2, FFF^-	F-F	0.100	0.539	0.000	0.199	0.015
3, $FClF^-$	F-Cl	0.099	0.257	0.000	0.254	−0.014
4, $ClFCl^-$	Cl-F	0.076	0.241	0.000	0.222	0.000
5, $[Cl_3]^-$	Cl-Cl	0.063	0.117	0.000	0.259	−0.006
6, H_2CSF_2	C-H	0.287	−1.022	0.004	1.371	−0.285
	C-S	0.262	−0.469	0.781	2.094	−0.354
	S-F	0.132	0.091	0.060	0.411	−0.069
7, ClF_3	P-F_e	0.201	0.033	0.149	0.511	−0.125
	P-F_a	0.156	0.234	0.115	0.363	−0.061
8, $[SF_3]^-$	S-F_e	0.160	−0.052	0.509	0.690	−0.137
	S-F_a	0.110	0.148	0.270	0.366	−0.040
9, F_4S	S-F_a	0.170	−0.062	0.068	0.589	−0.133
	S-F_e	0.205	−0.062	0.041	0.568	−0.226
10, F_4SO	S-O	0.312	1.140	0.139	0.250	−0.386
	S-F_a	0.194	−0.204	0.027	0.794	−0.202
	S-F_e	0.208	−0.102	0.050	0.612	−0.233
11, F_2PH_3	P-F	0.130	0.387	0.000	0.233	−0.085
	P-H	0.184	−0.113	0.001	0.618	−0.191
12, F_3PH_2	P-F_e	0.164	0.759	0.018	0.218	−0.101
	P-F_a	0.141	0.477	0.095	0.240	−0.095
	P-H	0.190	−0.148	0.034	0.667	−0.202
13, PF_5	P-F_e	0.173	0.812	0.053	0.221	−0.112
	P-F_a	0.164	0.645	0.000	0.228	−0.115
14, $[SiF_5]^-$	Si-F_e	0.116	0.808	0.034	0.174	−0.024
	Si-F_a	0.110	0.682	0.000	0.177	−0.028
15, F_6S	F-S	0.210	−0.127	0.000	0.627	−0.242
16, FH	F-H	0.369	−2.799	0.000	1.252	−0.784
17, F_2	F-F	0.267	0.594	0.000	0.352	−0.119
18, Cl_2	Cl-Cl	0.134	0.022	0.000	0.470	−0.052
19, FCl	F-Cl	0.182	0.061	0.000	0.452	−0.108
20, FPH_2	P-F	0.139	0.487	0.083	0.235	−0.088
	P-H	0.167	−0.130	0.202	0.745	−0.168
21, F_3P	F-P	0.157	0.620	0.070	0.232	−0.102
22, F_4Si	F-Si	0.138	1.120	0.000	0.164	−0.026
23, F_2S	F-S	0.177	0.001	0.568	0.610	−0.173

According to the above-mentioned trends, the structures can be classified in three main groups. One has structures **10–15** without lone pairs on the central atom, in which the axial/equatorial fluorine bonds had similar behavior for the geometries and electronic properties. The second group (**6–9**) has marked differences in the axial/equatorial geometries and electronic properties. For these structures, the differences may be due to the axial/equatorial bonding nature or to the electronic environment. In the third group, linear structures **1–5** have markedly different properties compared to the parent compounds (**16–19**). Among the three groups, the latter displayed characteristics compatible with the 3c-4e bond scheme.

For a qualitative as well as quantitative evaluation of the 3c-4e bond, the electron localization and delocalization indexes [21] were calculated, and the numerical values are presented in Table 2. In addition, a topological ELF study was also made, including the numerical populations and fluctuations for the different basins, to evaluate the electronic delocalization for these structures (see Table 3).

The Rundle [7] and Pimentel [8] 3c-4e bond model has a non-bonding Ψ_2 MO with two electrons (see Fig. 1). Therefore, an electron delocalization between the terminal nuclei should appear in this model. Compounds **10–15** (above-mentioned group 1) with a bipyramidal structure, displayed linear F-X-F moiety and a 3c-4e bond has been assigned, particularly for **13** (PF_5). Compounds **10**–**14** displayed two different bonding schemes for the axial/equatorial bonds, with the 3c-4e for the axial ones and three 2c-2e for the equatorial ones. In contrast, the bonding scheme in **15** was previously described in the literature as three 3c-4e bonds with an additional bonding MO [2b], resulting in six equivalent F-S bonds. Compounds **13** and **14** displayed D_{3h} symmetry with three equivalents equatorial bonds and two axial ones. The theoretical axial/equatorial bond lengths are similar with longer axial distances. Furthermore, as previously mentioned, all the geometrical and electronic properties were similar. In addition, the localization and delocalization indexes for both bonds were equivalent [$F(F_a,F_a) = 9.21$ and $F(F_e,F_e) = 9.20$ e^- for **13**]. In general, the delocalization indexes were very similar with larger values for the X-F_e bonds. On the other hand, the electron population of the ELF valence basins had the same trends [$V(Si,F_e) = 1.24$ and $V(Si,F_a) = 1.18$ e^- for **14**] and the monosynaptic valence basins at the fluorine-atom populations (lone pairs) were also similar and independent of the axial/equatorial nature for **13** and **14**. In addition, the

Table 2. Atomic localization index, F(A,A), and delocalization index δ(A,B)

A	F(A,A)	(%)[a]	A,B	δ(A,B)	A	F(A,A)	(%)[a]	A,B	δ(A,B)
1, FHF^-; ·· F	9.59	97.4	F,H	0.28	**12**, F_3PH_2; ·· P	10.35	88.2	P,F_a	0.48
H	0.04	12.3	F,F	0.22	F_a	9.27	95.0	P,F_e	0.54
2, FFF^-; ·· F_t	9.96	94.7	F_t,F_c	0.71	F_e	9.24	94.8	P,H	0.64
F_c	8.38	92.2	F_t,F_t	0.29	H	0.99	65.7	F_a,F_a	0.03
3, $FClF^-$; ·· F	9.15	95.2	F,F	0.15				F_e,F_a	0.17
Cl	15.99	95.3	Cl,F	0.78				F_a,H	0.06
4, $ClFCl^-$; ·· Cl	16.76	96.6	Cl,F	0.70				F_e,H	0.15
F	8.64	92.5	Cl,Cl	0.42	**13**, PF_5; ·· P	10.15	89.3	P,F_a	0.44
5, $[Cl_3]^-$; ·· Cl_t	16.94	97.0	Cl_t,Cl_c	0.79	F_a	9.21	94.6	P,F_e	0.51
Cl_c	16.27	95.4	Cl_t,Cl_t	0.27	F_e	9.20	94.7	F_a,F_a	< 0.01
6, H_2CSF_2; ·· S	12.88	88.4	S,C	1.76				F_e,F_e	0.06
F	9.08	94.4	S,F	0.77				F_a,F_e	0.20
C	4.54	69.7	C,H	0.93	**14**, SiF_5^-; ·· Si	10.0	92.8	Si,F_a	0.28
H	0.32	38.1	F,F	0.09	F_a	9.45	95.9	Si,F_e	0.33
			C,F	0.16	F_e	9.45	96.1	F_a,F_a	< 0.01
7, ClF_3; ·· Cl	14.41	91.0	Cl,F_a	0.91				F_e,F_e	0.05
F_a	8.84	93.7	Cl,F_e	1.05				F_e,F_a	0.17
F_e	8.62	92.8	F_a,F_a	0.15	**15**, F_6S; ·· S	10.68	84.4	S,F	0.66
			F_e,F_a	0.14	F	8.93	93.4	F_a,F_a	< 0.01
8, $[SF_3]^-$; ·· S	13.86	91.9	S,F_e	0.93				F_e,F_a	0.15
F_e	9.00	94.0	S,F_a	0.76	**16**, FH; ·· F	9.44	97.3	F,H	0.52
F_a	9.19	95.1	F_a,F_a	0.08	H	0.04	13.1		
			F_a,F_e	0.11	**17**, FF; ·· F	8.37	93.1	F,F	1.25
9, F_4S; ·· S	12.14	87.9	S,F_e	0.86	**18**, ClCl; ·· Cl	16.34	96.1	Cl,Cl	1.32
F_e	8.90	93.3	S,F_a	0.81	**19**, FCl; ·· F	8.74	93.5	F,Cl	1.21
F_a	8.97	93.9	F_a,F_a	0.06	Cl	16.05	96.4		
			F_e,F_e	0.11	**20**, FPH_2; ·· P	12.03	90.9	P,F	0.73
			F_a,F_e	0.15	F	9.27	95.1	P,H	0.84
10, F_4SO; ·· S	10.72	84.3	S,O	1.23	H	0.97	64.5	F,H	0.11
F_a	8.93	93.5	S,F_e	0.73				H,H	0.12
F_e	8.88	93.2	S,F_a	0.65	**21**, F_3P; ·· P	11.73	91.7	P,F	0.71
O	8.21	89.7	F_a,F_a	< 0.01	F	9.23	94.8	F,F	0.15
			F_e,F_e	0.06	**22**, F_4Si; ·· Si	9.99	92.5	Si,F	0.40
			F_a,F_e	0.19	F	9.43	96.2	F,F	0.12
			O,F_a	0.21	**23**, F_2S; ·· S	13.87	93.0	F,S	1.04
			O,F_e	0.11	F	8.96	93.9	F,F	0.13
11, F_2PH_3; ·· P	10.45	87.6	P,F	0.48					
F	9.31	95.3	P,H	0.66					
H	0.99	65.5	F,F	0.04					
			H,H	0.05					
			F,H	0.13					

[a] Percentage of electron localization = $(F(A,A)/N_A) \times 100\%$

overall electronic localization trends for the axial/equatorial bonds were highly similar to the parent compounds (**21** and **22**). For compounds **13** and **14,** non-electron delocalization was found between the axial fluorines, with only an axial/equatorial delocalization similar in magnitude to the $\delta(F_1,F_2)$ in the parent compounds.

Similar observations resulted analyzing the fluctuation contributions of the ELF valence basins in the V(F) basins (see Table 3), with an extremely small axial-axial contribution (< 1%).

Compounds **10** and **15** had sulfur as the central atom and the localization characteristic for the fluorine in **15** and both F_a and F_e in **10** had the same values (*ca.* 8.9 e^-). Analogous behavior was found for the remaining compounds in this group (**11** and **12**), including no electron delocalization between axial atoms.

From all the above electronic localization and delocalization results, we conclude that there is no evidence to support the 3c-4e model in the F_a-X-F_a substructure of this group, in agreement with Häser's results based on a one center-expansion technique for the PF_5 molecule [22d]. The small differences found between the axial/equatorial bonds are explained by the different chemical surroundings for these bonds.

The second group of compounds (**6–9**) displayed different T-shaped geometries with lone pairs on the central atom. These structures presented marked differences in the chemical axial/equatorial properties (bond lengths, charges and chemical shifts), the differences in the localization and delocalization for these structures between the axial/equatorial bonds were now not negligible with an increase in the $\delta(F_a,F_a)$ values from 0.06 in **9** to 0.15 in **7**. The $V(F_a)$ basin fluctuation contributions from the other axial basins also have larger values than in the former group (*ca.* 2%). These results support a small contribution to these structures of the 3c-4e model, due mainly to a slight electron delocalization between the axial fluorine atoms. However, the different behavior of the axial/equatorial atoms

Table 3. Basin population, N, variance, σ^2 and contribution fluctuations

		$\bar{N}$	σ^2	Contribution fluctuations (%)			$\bar{N}$	σ^2	Contribution fluctuations (%)
1, FHF^-	V(H)	0.30	0.26	29 V(F); 19 V(F→)	12, F_3PH_2	V(P,H_1)	2.10	0.58	13.5 V(P,H_2); 8 V(F_e); 6 V(P,F_e); 16 V(F_2); 8 V(P,F_2)
	V(F_1→)	0.94	0.66	8 V(H); 80 V(F_1); 3.2 V(F_2); 2.1 V(F_2→)		V(P,F_e)	1.15	0.81	4 V(P,H); 86 V(F_e); 3 V(F_2); 3 V(P,F_2)
	V(F_1)	6.76	1.02	8 V(H); 52 V(F_1→); 5.3 V(F_2); 2 V(F_2→)		V(P,F_2)	0.95	0.70	7 V(P,H); 3 V(F_e); 3 V(P,F_e); 69 V(F_2)
2, FFF^-	V(F_1)$_c$	6.93	1.03	32 V(F_2)		V(F_e)	6.68	1.37	2 V(P,H); 58 V(F_e); 20 V(P,F_e); 2 V(F_2); 1 V(P,F_2)
	V(F_2)$_t$	7.33	0.85	39 V(F_1); 15.6 V(F_3)		V(F_2)	6.81	1.35	3 V(P,H); 1.5 V(F_e); 1 V(P,F_e); 62 V(F_2); 17 V(P,F_2)
3, $FClF^-$	V(F)	7.44	0.83	44.5 V(Cl); 8.1 V(F_2)	13, PF_5	V(P,F_1)$_e$	1.23	0.86	67 V(F_1); 3.5 V(P,F_2); 1.6 V(P,F_1); 3.6 V(F_2); 2 V(F_e)
	V(Cl)	6.68	1.32	28 V(F)		V(P,F_2)$_a$	1.14	0.81	3.5 V(F_1); 3.6 V(P,F_1); 66 V(F_2)
4, $ClFCl^-$	V(F)	7.15	1.03	32 V(Cl)		V(F_1)	6.58	1.36	57 V(F_1); 21 V(P,F_1); 3 V(F_2)
	V(Cl_1)	7.22	1.12	30 V(F); 17 V(Cl_2)		V(F_2)	6.75	1.20	2 V(F_1); 64 V(F_2)
5, Cl_3^-	V(Cl_1)	6.96	1.30	28 V(Cl_2)	14, SiF_5^-	V(Si,F_1)$_e$	1.24	0.85	74 V(F_1); 2.2 V(Si,F_2); 1 V(Si,F_e); 3 V(F_2)
	V(Cl_2)	7.33	1.09	35 V(Cl_1); 11 V(Cl_3)		V(Si,F_2)$_a$	1.18	0.81	2.5 V(F_1); 2.3 V(Si,F_1); 73 V(F_2)
6, H_2CSF_2	V(S,C)	2.67	1.31	37 V(S); 6 V(F)		V(F_1)$_e$	6.60	1.36	58 V(F_1); 22 V(Si,F_1)
	V(S)	3.78	1.67	29 V(S,C); 20 V(F)		V(F_2)$_a$	6.65	1.17	19 V(Si,F_2); 64 V(F_2); 2 V(F_1)
	V(F_1)	7.45	1.43	3 V(S,C); 11 V(S); 69 V(F_1); 1.4 V(F_2)	15, SF_6	V(S,F_1)	1.05	0.77	60 V(F_1); 4 V(S,F_2); 4 V(F_2)
7, ClF_3	V(F_1→)	0.15	0.14	62 V(F_1); 11 V(Cl); 8.5 V(Cl→)		V(F_1)	6.86	1.14	66 V(F_1); 11 V(S,F_1)
	V(F_1)	6.93	1.30	60 V(F_1); 3.5 V(F_1→); 6.5 V(Cl); 4 V(Cl→); 2 V(F_2)	16, FH	V(FH)	1.45	0.77	93 V(F)
	V(F_2)	7.26	1.40	7 V(Cl); 65 V(F_2); 2.5 V(F_3)		V(F)	6.41	1.06	68 V(F,H)
	V(Cl→)	0.27	0.25	41 V(F_1); 5 V(F_1→); 19 V(Cl); 3 V(F_2)	17, FF	V(F_1→)	0.08	0.08	54 V(F_1); 38 V(F_2); 3 V(F_2→)
	V(Cl)	2.82	1.26	14 V(F_1); 28 V(Cl); 4 V(Cl→); 16 V(F_2)		V(F_1)	6.78	0.97	4.3 V(F_1→); 54 V(F_2); 3 V(F_2→)
8, SF_3^-	V(S,F_1)	0.40	0.35	59 V(F_1); 13 V(S); 2.5 V(F_2)	18, ClCl	V(Cl_1→)	0.36	0.31	50 V(Cl_1); 30 V(Cl_2); 11 V(Cl_2→)
	V(S)	2.45	1.50	15 V(F_1); 4 V(S,F_1); 27 V(S_2); 16 V(F_2)		V(Cl_1)	6.53	1.18	14 V(Cl_1→); 32 V(Cl_2); 8 V(Cl_2→)
	V(F_1)$_e$	7.17	1.40	68 V(F_1); 6.5 V(S,F_1); 5 V(S); 1.5 V(F_2)	19, FCl	V(F,Cl)	0.38	0.33	56 V(F); 36 V(Cl)

Table 3. Continued

		$\bar{N}$	σ^2	Contribution fluctuations (%)			$\bar{N}$	σ^2	Contribution fluctuations (%)
	$V(F_2)_a$	7.49	1.41	1.7 $V(F_1)$; 6 V(S); 71 $V(F_2)$; 1 $V(F_3)_a$		V(F)	6.93	1.00	19 V(F,Cl); 43 V(Cl)
9, F_4S	$V(S,F_3)_e$	0.89	0.68	9.5 V(S); 4 $V(S,F_e)$; 3 $V(S,F_a)$; 3.5 $V(F_a)$; 58 $V(F_3)$; 3.6 $V(F_e)$		V(Cl)	6.41	1.14	39 V(F); 11 V(F,Cl)
	$V(S,F_1)_a$	0.52	0.44	14.5 V(S); 5 $V(S,F_e)$; 56 $V(F_1)$	20, FPH_2	$V(P,H_1)$	2.00	0.58	26 $V(P,H_2)$; 37 V(P); 13 V(F); 6 V(P,F)
	V(S)	2.50	1.13	5.5 $V(S,F_e)$; 5.5 $V(S,F_a)$; 17 $V(F_a)$; 10 $V(F_e)$		V(P,F)	0.79	0.61	6 V(P,H); 9 V(P); 67 V(F)
	$V(F_3)_e$	6.88	1.37	4 V(S); 14.6 $V(S,F_3)$; 59.5 $V(F_3)$; 1.5 $V(F_e)$; 1.5 $V(F_a)$		V(P)	2.09	0.81	27 V(P,H); 15 V(F); 7 V(P,F)
	$V(F_1)_a$	7.18	1.40	7 V(S); 8 $V(S,F_1)$; 65 $V(F_1)$; 2 $V(F_e)$		V(F)	7.91	1.40	3 V(P,H); 60 V(F); 15 V(P,F)
10, F_4SO	$V(S,F_3)_e$	0.97	0.73	5 V(S,O); 2.6 $V(S,F_4)_e$; 9 $V(F_e)$; 4 $V(F_a)$; 58 $V(F_3)$; 5 $V(S,F_a)$	21, PF_3	$V(P,F_1)$	0.96	0.71	9 V(P); 67 $V(F_1)$; 3 $V(P,F_2)$; 3.5 $V(F_2)$
	$V(S,F_1)_a$	0.93	0.71	8 V(S,O); 5 $V(S,F_e)$; 57 $V(F_1)$; 5 $V(F_e)$		$V(F_1)$	6.80	1.40	6 V(P); 18 $V(P,F_1)$; 57 $V(F_1)$
	$V(F_3)_e$	6.84	1.37	15.6 $V(S,F_3)$; 1.5 $V(F_a)$; 59 $V(F_3)$		V(P)	2.23	0.85	7 V(P,F); 16 V(F)
	$V(F_1)_a$	6.93	1.23	11 $V(S,F_1)$; 69 $V(F_1)$	22, SiF_4	$V(Si,F_1)$	1.24	0.83	76 $V(F_1)$; 1.4 $V(Si,F_2)$
11, F_2PH_3	$V(P,H_1)$	2.07	0.58	17 $V(P,H_2)$; 8 V(P,F); 15 V(F)		$V(F_1)$	6.33	1.09	63 $V(F_1)$; 20 $V(Si,F_1)$; 1 $V(F_2)$; 2.5 $V(F_2)$
	$V(P,F_1)$	0.87	0.65	6.5 V(P,H); 69 $V(F_1)$; <1 $V(P,F_2)$	23, SF_2	V(S,F)	0.58	0.48	62 V(F); 12 V(S); 1.5 $V(S,F_2)$; 2.5 $V(F_2)$
	$V(F_1)$	6.85	1.10	2.5 V(P,H); 13 $V(P,F_1)$; 35 $V(F_1)$; <1 $V(F_2)$		V(F)	6.95	1.35	61 V(F); 10.5 V(S,F); 6 V(S); 1.5 $V(F_2)$
						V(S)	2.29	0.94	17 V(F); 6 V(S,F); 30 $V(S_2)$

[a] Arrows indicate a nonsynaptic basin directed to the joined atom

arose mainly from their different chemical surroundings (lone pairs).

The linear structures presented the largest overall differences compared to **16**–**19**. The localization indexes were highly different, and the delocalization ones between the terminal atoms were larger with values in the 0.15–0.42 range between terminal atoms, for **3** and **4**. The latter showed a noticeable electron delocalization. The delocalization observed in the linear compounds (**1**–**5**) is reflected also in the ELF fluctuation contributions values between the terminal basins, e.g., a value of 17% for **4**. This delocalization observed for the linear compounds strongly supports the 3c-4e model, in agreement with previous results [17a].

4 Conclusions

Theoretical calculations (B3LYP/6–311++G**) were performed on different structures, showing three-center linear and pseudo-linear arrangements. The compounds studied represented linear, T-shaped, and bipyramidal structures, with the latter group lacking electron pairs on the central atom. The electronic behavior of the $\rho(r)$ topology yielded the fluorine bonds to the central atom with a highly ionic character. The overall geometrical and electronic characteristics, including the electron delocalization indexes for the bipyramidal compounds (**10**–**15**), are similar for the axial and equatorial bonds. In addition, no electron delocalization was found between the axial fluorines for these compounds. Consequently, no 3c-4e bond scheme exists for these structures. However, the electron delocalization increased for the T-shaped (**5**–**9**) and linear (**1**–**5**) structures, indicating a participation of the 3c-4e model. The T-shaped structures presented different geometrical as well as electronic behavior between axial/equatorial bonds with a small amount of electron delocalization between axial atoms, and consequently a small contribution for the 3c-4e model. However, the linear structures showed larger differences in the geometry, compared with their parent compounds, and maximum electron delocalization values (with a noticeable value of 0.42 electron pairs for **4**) compatible with the 3c-4e bond model.

Acknowledgments. Computing time was provided by the Universidad de Granada (Spain). We are grateful to Professors R.F.W. Bader and B. Silvi for a copy of the AIMPAC and TopMoD package of programs. We thank Professor E. Sanchez Marcos for their fruitful discussion on the manuscript. We also thank D. Nesbitt for reviewing the language of the English manuscript.

References

1. Gilheany DG (1994) Chem Rev 94: 1339
2. (a) Akiba K (1999) In: Akiba K (ed), Chemistry of hypervalent compounds. Wiley-VCH: New York; (b) Curnow OJ (1998) J Chem Educ 75: 910
3. (a) Dobado JA, Martínez-García H, Molina J, Sundberg MR (1998) J Am Chem Soc 120: 8461; (b) Dobado JA, Martínez-García H, Molina J, Sundberg MR (1999) J Am Chem Soc 121: 3151
4. (a) Dobado JA, Martínez-García H, Molina J, Sundberg MR (2000) J Am Chem Soc 122: 1144; (b) Dobado JA, Martínez-García H, Molina J (1999) J Inorg Chem 38: 6257
5. (a) Reed AE, Weinhold F (1986) J Am Chem Soc 108: 3586; (b) Magnusson E (1990) J Am Chem Soc 112: 7940; (c) Reed AE, Schleyer PvR (1990) J Am Chem Soc 112: 1434; (d) Suidan L, Badenhoop JK, Glendening ED, Weinhold F (1995) J Chem Educ 72: 583; (e) Kutzelnigg W (1984) Angew Chem Int Ed Engl 23: 272
6. (a) Ciowsloski J, Surján PR (1992) Theochem 255: 9; (b) Cioslowski J, Mixon ST (1993) Inorg Chem 32: 3209.
7. (a) Hach RJ, Rundle RE (1951) J Am Chem Soc 73: 4321; (b) Rundle RE (1963) J Am Chem Soc 85: 112
8. Pimentel GC (1951) J Chem Phys 19: 446
9. Bilham J, Linnett JW (1964) Nature 201: 1323
10. Cooper DL, Cunningham TP, Gerratt J, Karadakov PB, Raimondi M (1994) J Am Chem Soc 116: 4414
11. (a) Bader RFW (1990) Atoms in Molecules: a Quantum Theory. Clarendon Press: Oxford; (b) Bader RFW (1991) Chem Rev 91: 893
12. Bader RFW, Johnson S, Tang T-H, Popelier PLA (1996) J Phys Chem 100: 15398
13. (a) Silvi B, Savin A (1994) Nature 371: 683; (b) Savin A, Nesper R, Wengert S, Fässler TF (1997) Angew Chem Int Ed Engl 36: 1809 (c) Marx D, Savin A (1997) Angew Chem Int Ed Engl 36: 2077
14. Becke AD, Edgecombe KE (1990) J Chem Phys 92: 5397
15. Bachrach SM (1994) In: Lipkowitz KB, Boyd DB (eds), Reviews in Computational Chemistry. VCH: New York, vol. 5, pp 171–227, and references cited therein
16. Ángyán JG, Loos M, Mayer I (1994) J Phys Chem 98: 5244 and references cited therein; (b) Ángyán JG, Rosta E, Surján PR (1999) Chem Phys Lett 299: 1 and references cited therein
17. (a) Kar T, Sánchez Marcos E (1992) Chem Phys Lett 192: 14; (b) Ponec R, Mayer I (1997) J Phys Chem A 101: 1738
18. Ponec R, Strand M (1994) Int J Quantum Chem 50: 43
19. Wiberg KB (1968) Tetrahedron 24: 1024
20. Bader RFW, Stephens ME (1975) J Am Chem Soc 97: 7391
21. Fradera X, Austen MA, Bader RFW (1999) J Phys Chem A 103: 304
22. (a) Fujimoto H, Yabuki R, Tamao K, Fukui K (1992) Theochem 260: 47; (b) Ziegler T, Gutsev GL (1992) J Chem Phys 96: 7623; (c) Moc J, Morokuma K (1994) Inorg Chem 33: 551; (d) Häser M (1996) J Am Chem Soc 118: 7311; (e) King RA, Galbraith JM, Schaefer III HF (1996) J Phys Chem 100: 6061; (f) Landrum GA, Goldberg N, Hoffmann R (1997) J Chem Soc Dalton Trans 3605; (g) Moc J, Morokuma K (1997) J Mol Struct 436: 401; (h) Ponec R, Duben AJ (1999) J Comput Chem 20: 760; (j) Fuster F, Silvi B (2000) Theor Chem Acc 104: 13
23. Gillespie RJ, Robinson EA (1996) Angew Chem Int Ed Engl 35: 495
24. Frisch MJ, Trucks GW, Schlegel HB, Scuseria GE, Robb MA, Cheeseman JR, Zakrzewski VG, Montgomery Jr JA, Stratmann RE, Burant JC, Dapprich S, Millam JM, Daniels AD, Kudin KN, Strain MC, Farkas O, Tomasi J, Barone V, Cossi M, Cammi R, Mennucci B, Pomelli C, Adamo C, Clifford S, Ochterski J, Petersson GA, Ayala PY, Cui Q, Morokuma K, Malick DK, Rabuck AD, Raghavachari K, Foresman JB, Cioslowski J, Ortiz JV, Baboul AG, Stefanov BB, Liu G, Liashenko A, Piskorz P, Komaromi I, Gomperts R, Martin RL, Fox DJ, Keith T, Al-Laham MA, Peng CY, Nanayakkara A, Gonzalez C, Challacombe M, Gill PMW, Johnson B, Chen W, Wong MW, Andres JL, Gonzalez C, Head-Gordon M, Replogle ES, Pople JA (1998) Gaussian 98, Revision A.7. Gaussian, Inc., Pittsburgh PA
25. Biegler-König FW, Bader RFW, Tang T-H (1982) J Comput Chem 3: 317
26. Wolinski K, Hilton JF, Pulay P (1990) J Am Chem Soc 112: 8251
27. MORPHY98, a program written by Popelier PLA with a contribution from Bone RGA, UMIST, Manchester England, EU (1998)
28. Noury S, Krokidis X, Fuster F, Silvi B (1997) ToPMoD package, Université Pierre et Marie Curie